Available online at www.sciencedirect.com
ScienceDirect
Trans. Nonferrous Met. Soc. China 35(2025) 1168−1181
Transactions of Nonferrous Metals Society of China
www.tnmsc.cn

Influence of γ' volume fraction on creep of Ni-based superalloy through phase-field simulations

Min YANG, Fan YANG, Jia CHEN, Min GUO, Hai-jun SU, Jun ZHANG

State Key Laboratory of Solidification Processing, Northwestern Polytechnical University, Xi'an 710072, China

Received 28 August 2023; accepted 10 May 2024

Abstract: γ' volume fraction (f_v) plays a critical role in the mechanical properties of Ni-based single-crystal superalloys. A creep phase-field model is utilized to simulate the microstructure evolution and creep performance during creep under different f_v conditions. The influence mechanism of f_v on creep properties is investigated based on the analysis of evolutions of internal stress and strain fields. As f_v increases, the morphology of γ' rafts changes from discontinuous to continuous, while the morphological change of γ channels is opposite, the inclination of γ channels from the [010] direction to ⟨011⟩ directions during tertiary creep first decreases and then increases, the creep life first increases and then decreases, and the main distribution of creep damage shifts from γ' to γ'/γ interfaces and γ channels. The longest creep life under f_v of 0.65 can be attributed to the stable γ' raft structure, the lowest stress and strain in γ channels, and the slowest damage accumulation.

Key words: phase-field simulation; internal stress; internal strain; creep behavior; single-crystal superalloys

1 Introduction

Ni-based single-crystal superalloys (Ni-SXs) have become preferred materials for turbine blades due to their excellent high-temperature creep properties [1−5]. The creep property is closely related to the microstructure. A large number of experimental studies have shown that the γ' size [6], the γ' volume fraction (f_v) [2,7], and the mismatch between γ' and γ phases [8] significantly influence the creep properties of Ni-SXs. Therefore, studying the relationship between the microstructure and creep properties of Ni-SXs and exploring the underlying mechanisms have always been the focal points of research.

Among these influencing factors, the γ' volume fraction plays a critical role in the creep properties. HARADA et al [9,10] conducted a series of experiments on the polycrystalline Ni-based superalloy Inconel 713C and found that the creep life of the alloy is the longest when f_v is around 65% under any creep condition. With the development of the Ni-SXs, this tendency is expected to be applicable to the Ni-SXs as well. MURAKUMO et al [7] studied the creep behavior of Ni-SXs with various f_v. The experimental results showed that under creep at 1173 K, 392 MPa and 1373 K, 137 MPa, the creep life is the longest when f_v is 70% and 55%, respectively. They inferred that Ni-SXs are strengthened by the γ'/γ interface rather than dispersed γ' precipitates. MUKHERJI et al [2] found that the creep life of a Ni-SX under 1273 K, 140−210 MPa conditions is higher when f_v is 0.58 compared to that when it is 0.50 or 0.65. They indicated that the change of creep properties with f_v is a result of the combined effect of γ'/γ interface strength and γ' coarsening. WU et al [11] studied the

Corresponding author: Jun ZHANG, Tel: +86-29-88492227, E-mail: zhjscott@nwpu.edu.cn;
Hai-jun SU, Tel: +86-29-88492227, E-mail: shjnpu@nwpu.edu.cn
DOI: https://doi.org/10.1016/S1003-6326(24)66741-5

effect of f_v (0.39 and 0.82) on creep behavior using a simulation method, and indicated that a high f_v is beneficial for the creep resistance of Ni-SXs. It is clear from the above research results that the optimal γ' volume fraction may depend on the creep condition, and the influence mechanism can be attributed to the γ'/γ interface strength.

The macroscopic creep deformation results from microscopic strains in the γ' and γ phases. Due to the different elastic/plastic parameters of γ' and γ phases, the internal stress and strain within the two phases are also different under creep stress. The variation of f_v will alter the distributions of internal stress and strain within the two phases, thereby influencing the creep properties. In addition, the internal stress and strain will in turn affect the evolutions of γ and γ' phases (such as γ' rafting) and ultimately the creep properties. Therefore, the microstructure-dependent internal stress/strain should also be considered one of the important factors for analyzing and understanding creep behavior. However, the changes of internal stress and strain fields under different f_v are still unclear, and there are very few studies on the effect of f_v on creep properties from the perspective of internal stress and strain fields.

Generally, it is extremely difficult to study the internal stress/strain at the microscale using experimental methods. With the rapid development of computer technology and numerical simulation, phase-field (PF) simulation has become a powerful method for studying the evolution mechanism of microstructures. A lot of work has been carried out to simulate the microstructure evolution and creep deformation of Ni-SXs using the PF method [12]. In these PF models, plastic deformation is typically coupled through slip system sliding [13−15] or dislocation motion [16,17], allowing for the simulation of microstructure evolution and creep deformation in the first two stages of creep. Recently, our group further incorporated creep damage and γ' shearing into the PF model (for convenience, this model is called the creep PF model), and realized simulations of γ'/γ evolutions and creep deformation throughout all three creep stages [18−20]. More recently, WU and ZHANG [21] proposed a phase-field model that also considers damage and γ' plastic deformation based on dislocation motion. The good consistency between simulation and experimental results indicates that the further modified PF model is applicable for understanding and predicting the microstructures and creep properties of Ni-SXs [18−21].

In this study, the creep PF model has been used to simulate the microstructure evolution and creep deformation with various f_v. By analyzing the evolutions of γ' and γ phases, as well as the changes in stresses, strains, and creep damage within the two phases under various f_v conditions, the influence mechanism of f_v on creep properties is intensively studied. These results can reveal the influence mechanism of f_v on creep behavior from the perspective of the evolutions of internal stress and strain fields, and provide theoretical guidance for designing the microstructure of superalloys with a high γ' volume fraction.

2 Creep PF model

A brief introduction of the creep PF model [18,19] is given here. A concentration field $c(\boldsymbol{r})$ of Al element and three long-range ordered (LRO) parameter fields $\eta_i(\boldsymbol{r})$ (i=1, 2, 3) are used to describe the γ' and γ phases. The evolutions of the two phases are governed by the Cahn−Hilliard equation and Allen−Cahn equations:

$$\frac{\partial c(\boldsymbol{r},t)}{\partial t}=M\nabla^2\frac{\delta F}{\delta c(\boldsymbol{r},t)} \tag{1}$$

$$\frac{\partial \eta_i(\boldsymbol{r},t)}{\partial t}=-L\frac{\delta F}{\delta \eta_i(\boldsymbol{r},t)},\ i=1,\ 2,\ 3 \tag{2}$$

where $c(\boldsymbol{r}, t)$ is the concentration field and $\eta_i(\boldsymbol{r}, t)$ is the long-range order (LRO) parameter field. $\boldsymbol{r}$ represents the position coordinates, t is time, and M and L are the diffusional mobility and the relaxation kinetics of LRO parameters, respectively. F is the total energy, which is the sum of non-equilibrium chemical free energy (F_{ch}), elastic strain energy (F_{el}) and plastic strain energy (F_{pl}), i.e., $F=F_{ch}+F_{el}+F_{pl}$.

F_{ch} is given by a standard Ginzburg−Landau function:

$$F_{ch}=\int_V\left[f\left(c,\eta_i\right)+\frac{\alpha}{2}\left|\nabla c\right|^2+\frac{\beta}{2}\sum_{i=1}^{3}\left|\nabla\eta_i\right|^2\right]\mathrm{d}V \tag{3}$$

where α and β are the constant gradient coefficients, and $f(c, \eta_i)$ represents the local free energy density.

The elastic strain energy (F_{el}) is calculated by micro-elasticity theory. The relevant calculation equations are as follows:

$$F_{\mathrm{el}}=\frac{1}{2}\int_V \lambda_{ijkl}(\boldsymbol{r})\varepsilon_{ij}^{\mathrm{el}}(\boldsymbol{r})\varepsilon_{kl}^{\mathrm{el}}(\boldsymbol{r})\mathrm{d}V \tag{4}$$

$$\lambda_{ijkl}(\boldsymbol{r})=\overline{\lambda}_{ijkl}+\Delta\lambda_{ijkl}\Delta c(\boldsymbol{r}) \tag{5}$$

$$\varepsilon_{ij}^{\mathrm{el}}(\boldsymbol{r})=\varepsilon_{ij}(\boldsymbol{r})-\varepsilon_{ij}^{\mathrm{o}}(\boldsymbol{r})-\varepsilon_{ij}^{\mathrm{pl}}(\boldsymbol{r}) \tag{6}$$

where $\lambda_{ijkl}(\boldsymbol{r})$ is the local elastic modulus and assigned as a function of concentration field. $\overline{\lambda}_{ijkl}$ is the average elastic modulus, $\Delta\lambda_{ijkl}$ is the difference between elastic moduli of γ' ($\lambda_{ijkl}^{\mathrm{p}}$) and γ ($\lambda_{ijkl}^{\mathrm{m}}$), $\varepsilon_{ij}^{\mathrm{el}}(\boldsymbol{r})$ is the elastic strain, $\varepsilon_{ij}(\boldsymbol{r})$ is the total strain, $\varepsilon_{ij}^{\mathrm{pl}}(\boldsymbol{r})$ is plastic strain and $\varepsilon_{ij}^{\mathrm{o}}(\boldsymbol{r})$ is the stress-free transform strain. $\varepsilon_{ij}^{\mathrm{o}}(\boldsymbol{r})$ is the function of concentration, i.e. $\varepsilon_{ij}^{\mathrm{o}}(\boldsymbol{r})=\varepsilon_{\mathrm{o}}\Delta c(\boldsymbol{r})\delta_{ij}$, where δ_{ij} is the Kronecker delta and $\varepsilon_{\mathrm{o}}=\delta/(c_{\mathrm{p}}-c_{\mathrm{m}})$. δ is the γ'/γ lattice misfit; c_{p} and c_{m} are equilibrium concentrations in γ' and γ, respectively.

The plastic deformation during creep at low and medium temperatures is dominated by dislocation slip [22]. Therefore, the crystal plastic theory is adopted to calculate the plastic strain energy [23]. The effect of creep damage on plastic deformation is considered to simulate tertiary creep, and the constitutive equations are as follows:

$$\dot{\boldsymbol{\varepsilon}}^{\mathrm{pl}}=\sum_s \boldsymbol{m}^s\dot{\gamma}^s,\quad \boldsymbol{m}^s=\frac{1}{2}(\boldsymbol{n}^s\otimes\boldsymbol{l}^s+\boldsymbol{l}^s\otimes\boldsymbol{n}^s) \tag{7}$$

$$\dot{\gamma}^s=\left\langle\frac{|\tau^s|-r^s-r_0}{K}\right\rangle^n \mathrm{sign}(\tau^s) \tag{8}$$

$$\tau^s=\frac{1}{1-\omega^s}\boldsymbol{\sigma}:\boldsymbol{m}^s \tag{9}$$

$$\dot{\omega}^s(\boldsymbol{r},t)=D_{\mathrm{a}}(\tau^s(\boldsymbol{r},t))^m \tag{10}$$

$$r^s=\sum_j H_{sj}b^jQ^jq^j,\quad \dot{q}^s=\left|\dot{\gamma}^s\right|\left(1-b^sq^s\right) \tag{11}$$

$$F_{\mathrm{pl}}=\int_V[1/2\sum_s b^sQ^s(q^s)^2]\mathrm{d}V \tag{12}$$

where $\dot{\boldsymbol{\varepsilon}}^{\mathrm{pl}}$ is the plastic strain rate and calculated based on the sum of slip accumulations of each slip system s. $\boldsymbol{m}^s$ is the orientation tensor, $\boldsymbol{n}^s$ is the slip plane, $\boldsymbol{l}^s$ is the slip direction, and $\dot{\gamma}^s$ is the plastic shear rate on the slip system s. Only octahedral slip systems are considered here. The resolved shear stress (τ^s) is a function of creep damage variable (ω^s) and Cauchy stress ($\boldsymbol{\sigma}$). When $\omega^s=0$, it represents an undamaged state. With the increase of local ω^s, the local stress concentration increases, accelerating the local plastic deformation. This induces a rapid rise in creep strain during the tertiary creep. When $\omega^s=1$, it represents a complete damage state, which corresponds to the formation of micro-voids and micro-cracks. r^s is the isotropic hardening and r_0 is an initial threshold for the activation of slip system. It should be noted that the initial threshold for γ' phase (r_0^{p}) is higher than that for γ matrix (r_0^{m}), to ensure that γ-channel plasticity is sustained during whole creep process, while γ' plasticity mainly occurs during the tertiary creep. H_{sj} is an interaction matrix of slip systems, and K, n, b^s, Q^s, D_{a} and m are the constant material parameters. The values of parameters used here are adopted for the superalloy AM1 at 1223 K and listed in Tables 1 and 2.

Table 1 Values of parameters used in creep PF model [18]

Parameter	Value
Equilibrium concentration in γ', c_{p}	0.231
Equilibrium concentration in γ, c_{m}	0.15
Gradient coefficient, α/(J·m^{-1})	2.5×10^{-9}
Gradient coefficient, β/(J·m^{-1})	6.3×10^{-12}
Material parameter, n	7.15
Material parameter, K/(MPa·s$^{1/n}$)	545
Material parameter, b^s	400
Material parameter, Q^s/MPa	10
Material parameter, m	2
Material parameter, D_{a}/MPa$^{1/m}$	1.3×10^{-20}
Initial threshold for γ, r_0^{m}/MPa	35
Initial threshold for γ', r_0^{p}/MPa	500
γ'/γ lattice misfit, δ	−0.001

Table 2 Elastic stiffness for γ and γ' phases [18]

Parameter	γ	γ'
C_{11}/GPa	197	193
C_{12}/GPa	144	131
C_{44}/GPa	90	97

A validation of the current creep PF model has been conducted by comparing the simulated and experimental creep microstructures and properties of a Ni−Al single-crystal alloy under various creep stresses. The comparison indicates that the creep PF model can reproduce the microstructure evolutions throughout the entire creep process, effectively simulate the performance changes during the first

two creep stages, and predict the influence of creep stress on creep properties. For more detailed information, please refer to Ref. [19].

3 Results

3.1 Microstructure evolutions during creep with various f_v

According to experimental results [7,9,10], four kinds of γ' volume fractions (f_v) are selected: 0.45, 0.55, 0.65 and 0.75. The γ' and γ evolutions during tensile creep at 1223 K, 300 MPa under four different f_v conditions are simulated. Considering the computational efficiency, the simulation domain is short in one of the three dimensions and its size is 80 nm × 1280 nm × 1280 nm. Due to the narrow size in the [100] direction, the microstructure is unchanged along this direction. Thus, the microstructure evolution within the section normal to the [100] direction is shown here (see Fig. 1). Generally, as creep time prolongs, the γ' phases are coarsened along the direction normal to the tensile axis, i.e. along the [010] direction, forming n-type rafting. In the case of f_v=0.45 (Figs. 1(a−d)), some γ' phases split into several pieces (as shown in the red-dashed box), to form γ' rafts and γ channels which are distributed along the [010] direction. Since f_v is low and the distance between neighboring γ' phases is relatively large, γ' rafts are discontinuous. As time increases, some rafted γ' phases become wavy, and the thickness of γ' rafts becomes thinner at certain positions, as shown in

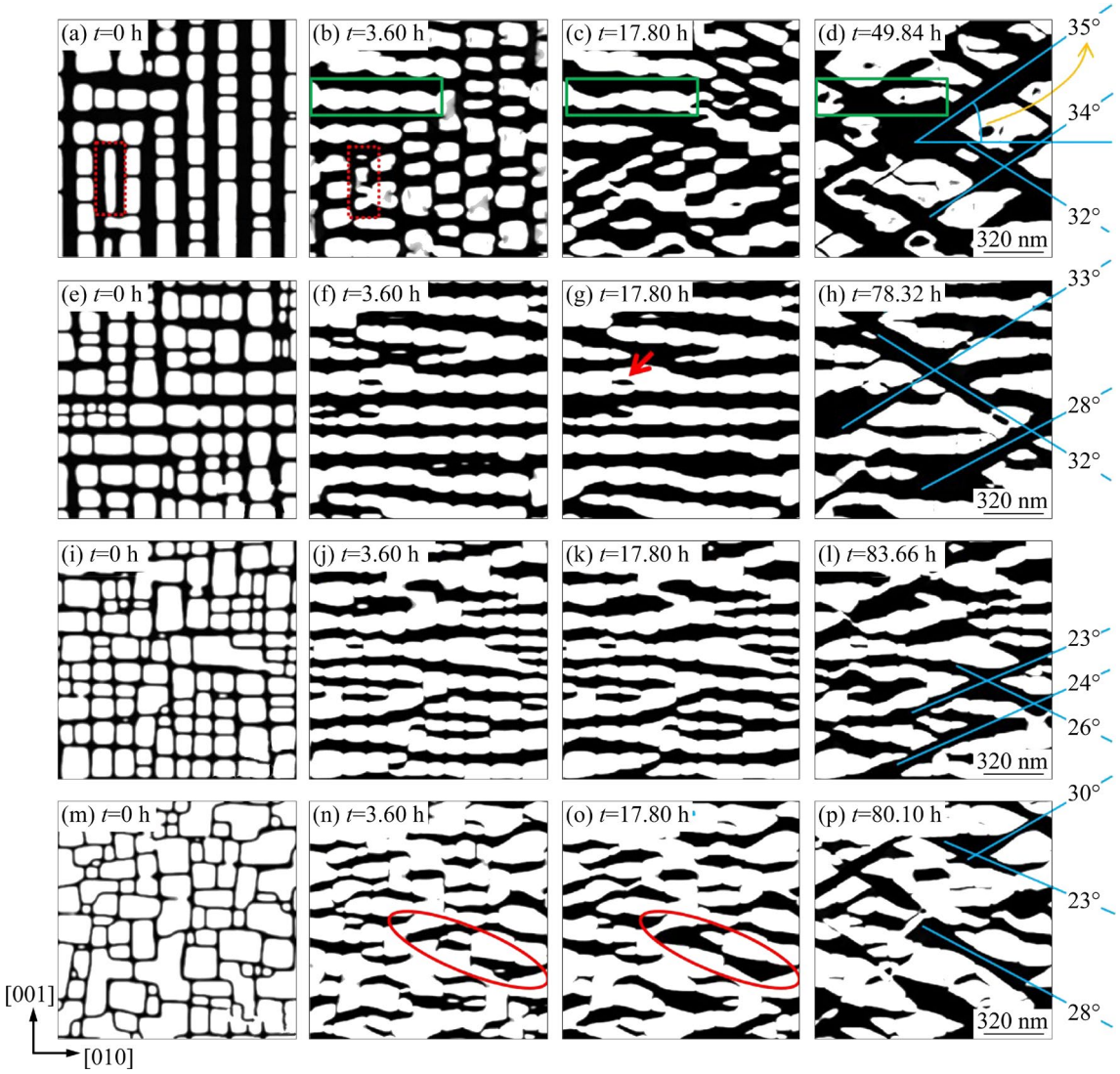

Fig. 1 Evolutions of γ' and γ phases during tensile creep at 1223 K, 300 MPa under different f_v conditions: (a−d) f_v=0.45; (e−h) f_v=0.55; (i−l) f_v=0.65; (m−p) f_v=0.75 (The applied stress is along the [001] direction; The rotated angle is measured between the orientation of γ channels and the horizontal direction)

the green box. The wave-shaped γ' rafts can also be observed in the experimental and other simulation results [1,18,21], which is the result of the accumulation of plastic deformation in γ and γ' phases. According to the elastic energy calculation by TANAKA et al [24], it is found that [001] raft structure is stabilized by a small amount of plastic deformation but becomes unstable when the plastic strain exceeds a certain value, resulting in the wave-shaped γ' rafts. Furthermore, the γ' rafts can disconnect at the thin positions, to form continuous γ channels which are titled to ⟨011⟩ directions, as shown in the green box. At the end of creep, the γ' rafts are severely coarsened and most γ channels rotate from ⟨001⟩ directions to ⟨011⟩ directions. Similarly, ALI et al [25] reported that under high-stress conditions, the direction of γ channels shifts to 45° during creep. The essential reason for this rotation is the accumulation of high plastic strain. These simulation results are also in line with experimental results reported by TOURATIER et al [26].

When f_v=0.55 (Figs. 1(e−h)), the continuous γ' rafts as well as γ channels are formed during the creep. The island-like γ phase can be observed, as indicated by the red arrow. This island-like γ phase may disappear with the increase of creep time. In the later stage of creep, the continuous γ' rafts lose their stability, and part of γ channels deviate to the ⟨011⟩ directions.

The microstructure evolution in the case of f_v=0.65 is similar to that of f_v=0.55 (see Figs. 1(i–l)). It should be noted that at the end of creep, γ' rafts are still relatively continuous (see Fig. 1(l)). From the measured angles between the orientation of γ channels and the horizontal direction shown in Figs. 1(d, h, l), it can be observed that the rotation degree of γ channels decreases with increasing f_v. It is found that as the accumulation of plastic strain increases, a destabilization of the n-type or p-type γ' rafts occurs which progressively leads to the 45° γ' rafts [26]. The accumulated plastic deformation in the later stage of creep increases with f_v decreasing from 0.65 to 0.45 (see Fig. 2), increasing the rotation degree of γ channels.

When f_v=0.75 (see Figs. 1(m−p)), the high f_v causes neighboring γ' phases to connect massively, resulting in narrow and discontinuous γ channels. These γ' phases continue to coarsen during creep, and some short γ channels merge to form longer γ channels (as shown in the red ellipse). By the end of creep, the coarse γ' phases and wide γ channels are formed, and γ channels deviate to the ⟨011⟩ directions. A comparison between Figs. 1(l) and 1(p) reveals that the deviation degree of γ channels in the case of f_v=0.75 is greater than that in the case of f_v=0.65.

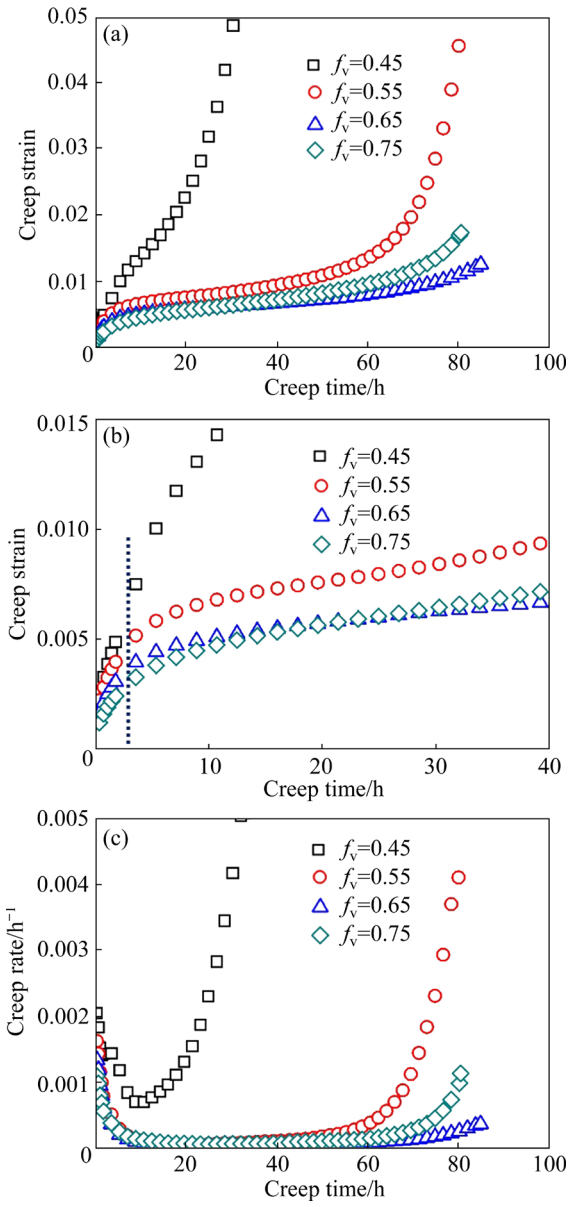

Fig. 2 Creep curves at 1223 K, 300 MPa with different f_v: (a) Creep strain curves; (b) Enlarged curves within initial 40 h in (a); (c) Creep rate curves

3.2 Creep curves under different f_v conditions

The creep curves under different f_v conditions are shown in Fig. 2. In all cases, the creep curve consists of three stages: primary, steady-state and tertiary creep. At the end of primary creep, the creep strain decreases with the increase of f_v (see

the dotted line region in Fig. 2(b)). This is because when f_v is lower, the width of γ channels is larger, which is conducive to the movement of dislocations and thus results in a higher plastic strain accumulation. However, in the steady-state creep, the monotonic relationship between creep strain and f_v is destroyed. As f_v increases, the creep strain first decreases and then increases. When f_v=0.65, the creep strain is the lowest. The reason for the alteration of the relationship is as follows. When f_v=0.75, although γ channels become shorter and discontinuous, the inclination degree of γ channels to the ⟨011⟩ directions increases, thereby enhancing the movement of dislocations. As a result, a higher steady-state creep rate and, consequently, a higher plastic strain appear under f_v=0.75 condition compared to f_v=0.65 condition. The creep lives for four cases are listed in Table 3. The creep life first increases and then decreases as f_v increases. When f_v=0.65, the creep life is the longest, which is consistent with the normal knowledge [9,10]. It is worth noting that the simulated performance trend is not as evident as the experimental performance trend. On the one hand, the microstructure evolution during creep is controlled by the energy fields (such as chemical free energy field, and elastic energy field) and diffusion of all alloying elements. In the present model, a simplified Ni−Al binary system model has been used, ignoring the influence of other elements on the microstructure evolution and creep property, such as Re which can reduce the diffusion rate of elements, delay the increase in γ channel thickness and therefore increase the creep resistance. This simplification may result in the difference between simulation and experimental results. On the other hand, from previous experimental validation of Ni−Al binary alloy [19], it is known that the present model can effectively simulate the performance changes during the first two creep stages, but is the shortage in the third creep stage, inducing the difference between simulation and experiments. In this work, the focus is on understanding the influence mechanism of f_v on creep, rather than precisely predicting the creep life change with different f_v. In addition, the creep life of superalloys mainly depends on the steady-state stage and the influence mechanism of f_v should be mainly limited to this stage. Therefore, using the present model is sufficient for study.

Besides, as mentioned in the Introduction, the creep life is the longest at 1173 K, 392 MPa [7], 1373 K, 137 MPa [7] and 1273 K, 140−210 MPa [2] when f_v is about 70%, 55% and 0.58, respectively. Based on these experimental and present simulation results, it can be concluded that the optimal γ' phase volume fraction for maximum creep life is dependent on temperature. This relationship is illustrated in Fig. 3. As the creep temperature increases, the optimal γ' volume fraction tends to decrease. Higher temperature can increase the atomic activity and accelerate the diffusion process, leading to a faster coarsening rate of γ' phases. Moreover, a larger f_v results in a shorter spacing between adjacent γ' phases, making it easier for them to connect and surround the γ matrix at high temperature, thereby reducing the creep resistance. Therefore, under a higher temperature condition, the optimal γ' phase volume fraction corresponding to the longest creep life is lower.

Table 3 Creep life at 1223 K, 300 MPa under different f_v conditions

f_v	0.45	0.55	0.65	0.75
Creep life/h	51.0	80.0	84.8	80.4

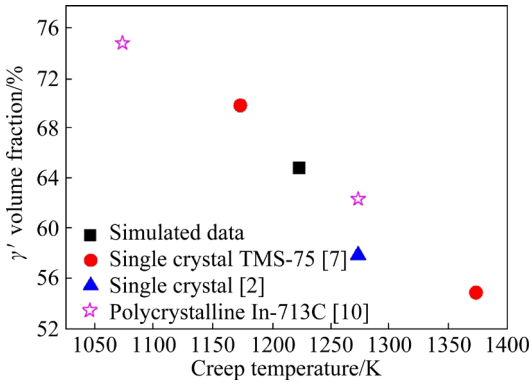

Fig. 3 Relationship between creep temperature and optimal γ' volume fraction corresponding to maximum creep life

When combining the microstructure evolution and creep curves, it is evident that during primary creep, γ' phases are coarsened directionally, forming γ' rafts. During steady-state creep, the rafted γ' phases continue coarsening and γ channels become wider and straighter. During tertiary creep, the rafted γ' phases keep coarsening and their shape becomes wavy. At the same time, the horizontal γ channels deviate to the ⟨011⟩ directions, along

with the local disconnection of γ' rafts, ultimately forming continuous γ channels in the ⟨011⟩ directions.

4 Discussion

4.1 Effect of f_v on creep properties

The effect of f_v on creep properties is primarily determined by its impact on the evolutions of the micro stress and strain fields. Therefore, it is crucial to analyzing the evolutions of these fields during creep.

For instance, when f_v=0.45, the evolutions of the equivalent stress, equivalent elastic strain and equivalent plastic strain fields are shown in Fig. 4. The initial stress in horizontal γ channels is higher than that in vertical γ channels, which is consistent with the findings of internal stress in γ' and γ phases by KAMARAJ et al [27], as well as the calculation results obtained through finite element method (FEM) by MÜLLER et al [28]. This uneven distribution of stress in γ channels is a result of the interaction between γ'/γ coherent misfit and external loading. The plastic strain is initially zero everywhere, as there is no plastic activity.

In primary creep, the plastic strain is only generated in γ channels and mainly concentrated in the horizontal channels. This is supported by experimental TEM investigations, which have shown that the deformation of negative misfit alloys under tensile creep begins in the horizontal channels [3,5]. Recently, SULZER et al [29] utilized high-resolution electron backscatter diffraction (HR-EBSD) and electron channeling contrast imaging under controlled diffraction conditions (cECCI) to study the evolutions of creep strain and dislocation density in Ni-SXs. The strain distribution (see Fig. 3 in Ref. [29]) clearly illustrates that the strain is localized within γ channels, with higher strain values being present in the horizontal γ channels. This concentrated distribution of plastic strain in horizontal γ channels is a direct result of the higher internal stress in these channels and the lower initial threshold of γ phases. Moreover, the distribution of plastic strain in γ channels is anisotropic, with high plastic strain mainly distributed along the ⟨011⟩ directions, i.e. slip directions of slip systems. This finding is consistent with other simulations [12,17,19,21]. The internal stress in horizontal γ channels (see Fig. 4(b)) is reduced compared to the initial state, because plastic deformation is able to release local stress concentration to a certain degree. In addition, the movement of dislocations in γ channels is hindered by γ'/γ interfaces, resulting in internal stress within γ' phases. Thus, the stress within γ' phases is higher

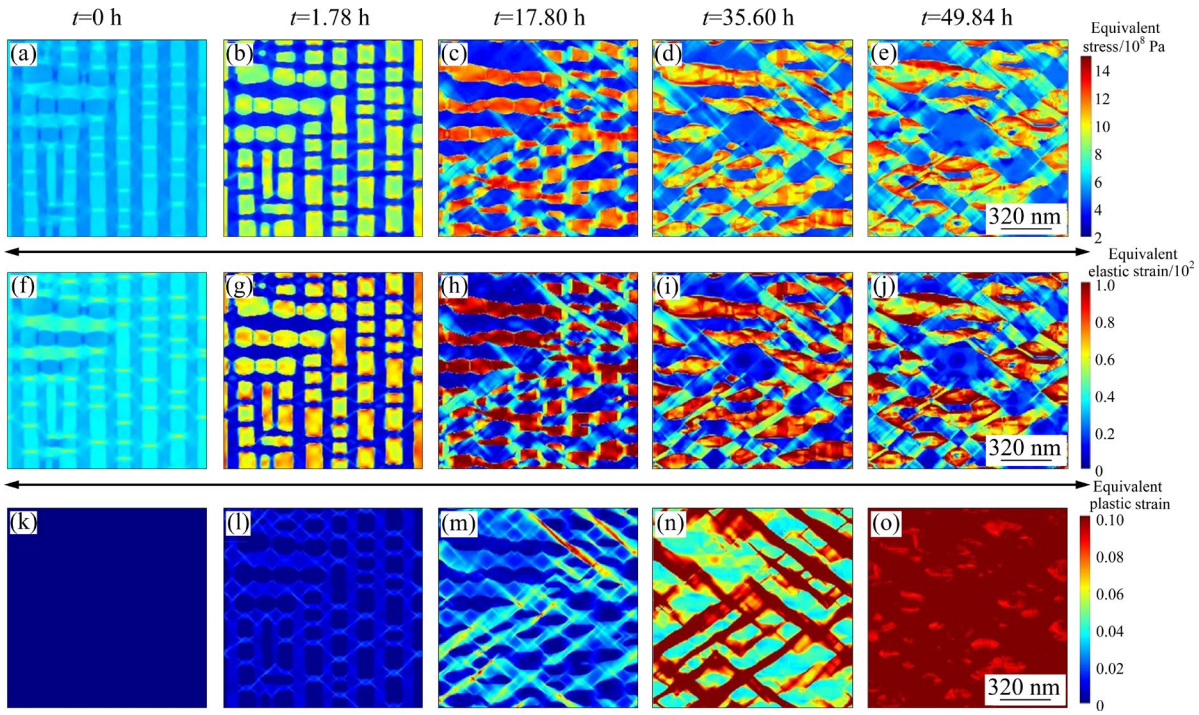

Fig. 4 Evolutions of equivalent stress field (a−e), equivalent elastic strain field (f−j) and equivalent plastic strain field (k−o) during creep at 1223 K, 300 MPa for f_v=0.45

than that within γ channels, and local stress concentration appears at the edge of γ' phases. The FEM calculation by MÜLLER et al [28] indicates that the stress is higher within γ' phase than within γ channel, and the stress in horizontal γ channel decreases rapidly compared to its initial state, consistent with the present simulation results

As creep time prolongs, the plastic strain continues to accumulate in γ channels (see Fig. 4(m) during the steady-state creep). A notable feature is that the distribution of plastic strain in γ channels is influenced by the local morphology of γ' rafts. In regions where γ' rafts are continuous, the dislocation movement in γ channels is easily hindered by the γ' rafts, resulting in a smaller amount of plastic strain. However, in regions where γ' rafts are discontinuous, this hindering effect is weakened. Some γ'/γ interfaces deviate to the $\langle 011 \rangle$ directions, causing the corresponding γ channels to also incline to the $\langle 011 \rangle$ directions. This facilitates dislocation movement and ultimately leads to a larger amount of plastic strain in γ channels. This non-uniform distributions of γ' morphology and plastic strain support the idea that the rotations of γ'/γ interface and γ channel are caused by the accumulation of high plastic strain, which is consistent with the analysis in Refs. [25,26]. Besides, as the plastic strain accumulates in γ channels, more and more slips are hindered by γ' phases, resulting in an increase of internal stress within γ' phases (see Figs. 4(b−c)). When the local resolved shear stress in γ' phases exceeds the initial threshold of γ' phase, plastic deformation occurs in γ' phases (see Fig. 4(m)). Another interesting feature is that the stress in γ channels in the continuous γ' rafting region is relatively lower than that in the discontinuous γ' rafting region (see Fig. 4(c)). The stress in γ channels can be released partly by the plastic deformation. However, the plastic deformation can also induce the creep damage which in turn can enhance the local stress concentration. Thus, the change of local stress is actually determined by a combined effect of plastic deformation and creep damage. In the continuous γ' rafting region, where plastic deformation is low, the local stress relaxation effect caused by the plastic deformation is stronger than the local stress strengthening effect caused by the creep damage, resulting in a decrease in stress with the accumulation of the plastic strain. However, in the discontinuous γ' rafting region, where plastic deformation is high, the stress strengthening effect outweighs the stress relaxation effect, leading to an increase in stress with the accumulation of plastic strain.

In the third stage of creep, a large amount of plastic strain accumulates in both γ' and γ phases (see Figs. 4(n−o)), and the stress turns to be obviously increased in γ channels but slightly decreased in γ' rafts (see Figs. 4(d, e)). As a result, the creep damage is exacerbated rapidly, leading to final creep rupture.

Generally, as the creep time increases, the plastic strain accumulates constantly, first within γ channels and then within both phases (see Figs. 4(k−o)); the stress in γ' phase initially increases and then may decrease; while the stress in γ channels for the most part first decreases and then increases (see Figs. 4(a−e)). The evolution trend of the elastic strain in γ channels and γ' phases is the same as that of the stress (see Figs. 4(f−j)) due to the proportional relationship between stress and elastic strain. Similar evolution trends of stress and strain fields within γ and γ' phases can be observed in the study by WU and ZHANG [21], where a model coupling phase-field, dislocation density-based plasticity and damage is used to simulate the microstructure evolution and creep deformation of Ni-SXs during creep.

The evolutions of the equivalent stress field and equivalent plastic strain field during creep for cases of f_v=0.55, 0.65 and 0.75 are shown in Figs. 5−7, respectively. In the cases of f_v=0.55 and 0.65 where the γ' rafts are relatively continuous, the plastic strain varies with the width of horizontal γ channels (see Figs. 5 and 6). In areas with wider γ channels, the accumulated plastic strain is higher due to easier movement of dislocations. SULZER et al [29] plotted the average geometrically necessary dislocation (GND) density map of creep microstructure and found that the GND density is uneven, with high GND density emerging in areas with locally wider γ channels. This means that the high plastic strain is generated in locally wider γ channels, which is consistent with the present simulation results. The evolution trends of stress and strain fields for cases of f_v=0.55, 0.65 and 0.75 are similar to those for the case of f_v=0.45. However, as f_v increases from 0.45 to 0.75, the distributions of stress and strain within γ' and γ phases are changed

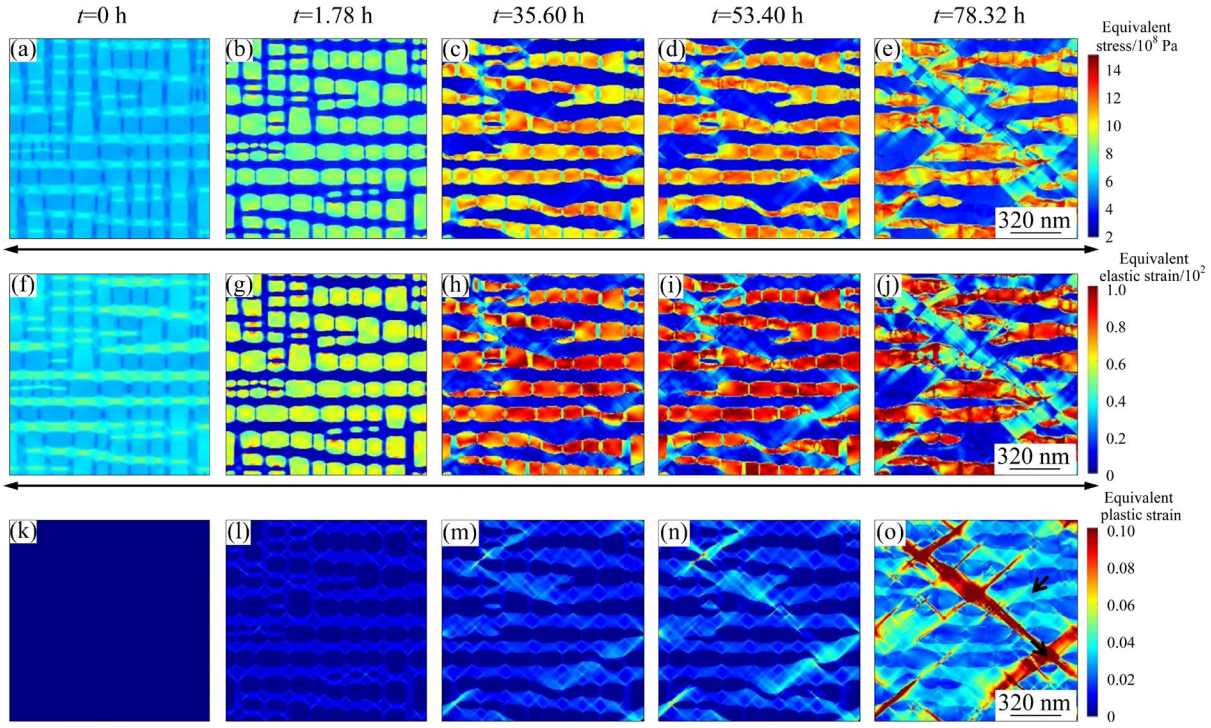

Fig. 5 Evolutions of equivalent stress field (a−e), equivalent elastic strain field (f−j) and equivalent plastic strain field (k−o) during creep at 1223 K, 300 MPa for f_v=0.55

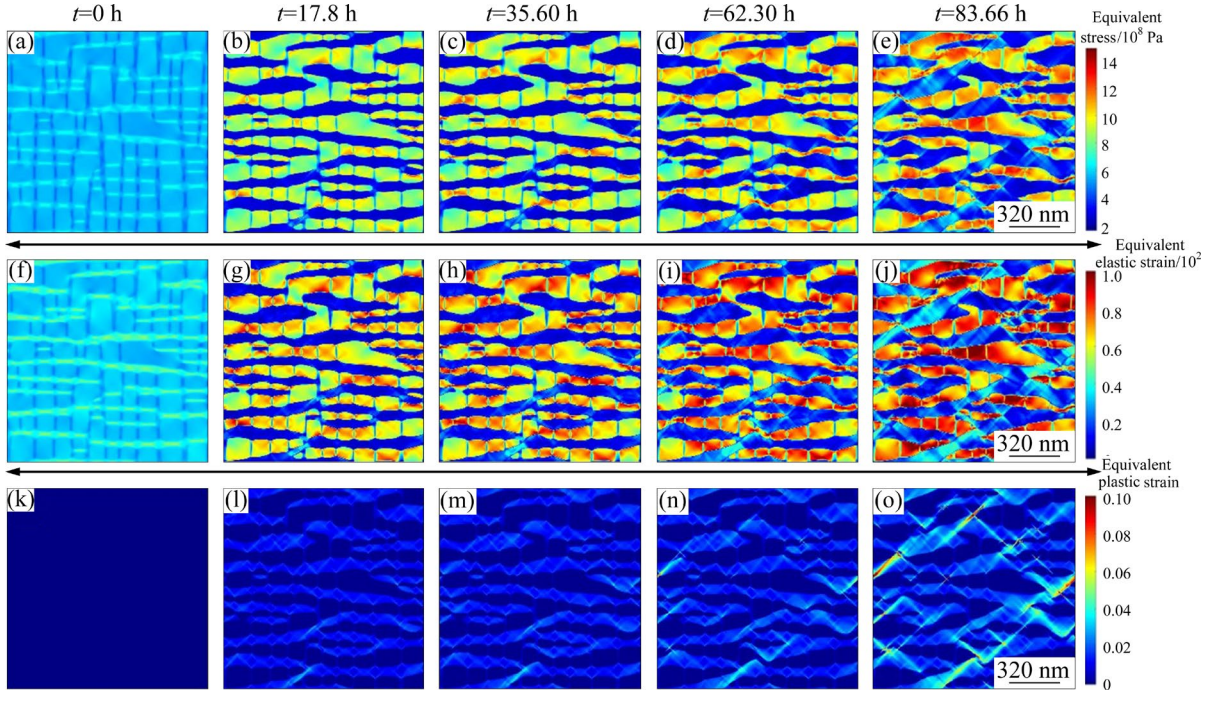

Fig. 6 Evolutions of equivalent stress field (a−e), equivalent elastic strain field (f−j) and equivalent plastic strain field (k−o) during creep at 1223 K, 300 MPa for f_v=0.65

significantly. For a clear comparison, the equivalent stress field and equivalent strain field at the same creep time (during the steady-state stage) for all cases are shown in Fig. 8. The relationship between the mean stress/strain in γ' and γ phases with f_v is shown in Fig. 9. The following points can be drawn from Figs. 8 and 9: (1) as f_v increases, the mean stress within γ' phases gradually decreases, while

the mean stress in γ channels first decreases and then increases; (2) the change trends of the mean elastic strain in γ' and γ phases are the same as those of the mean stress; (3) the mean plastic strain in γ channels and γ' phases first decreases and then increases; (4) when f_v=0.65, the mean stress, mean elastic strain and mean plastic strain in γ channels are in the lowest state.

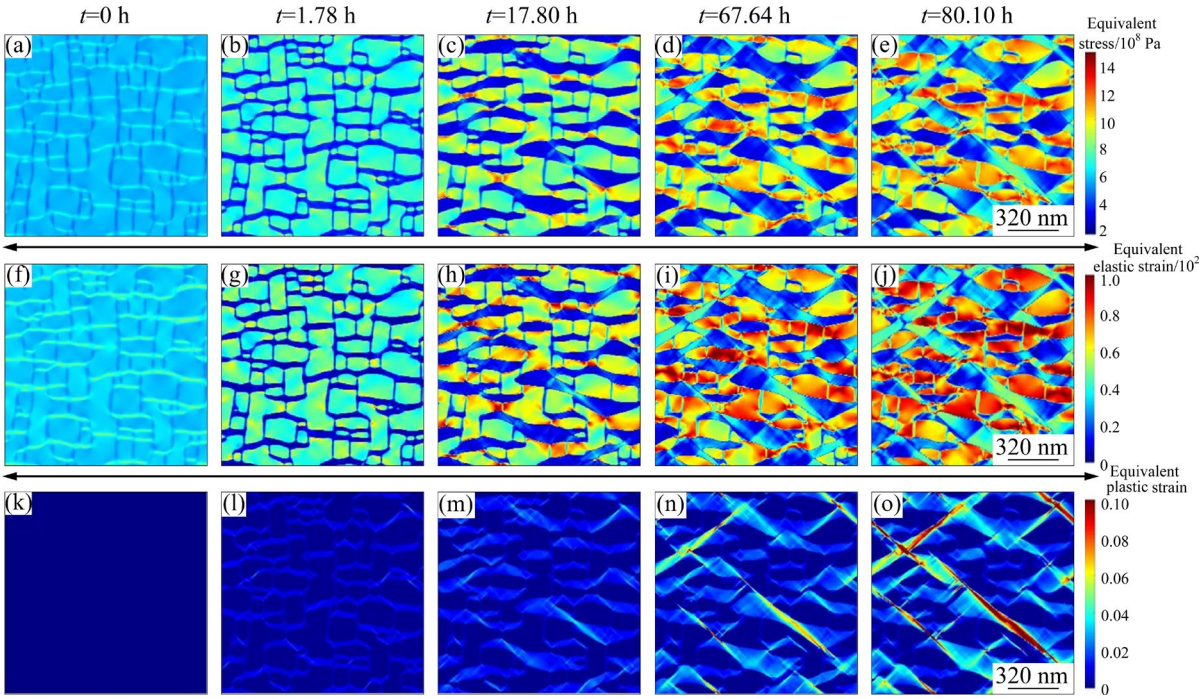

Fig. 7 Evolutions of equivalent stress field (a−e), equivalent elastic strain field (f−j) and equivalent plastic strain field (k−o) during creep at 1223 K, 300 MPa for f_v=0.75

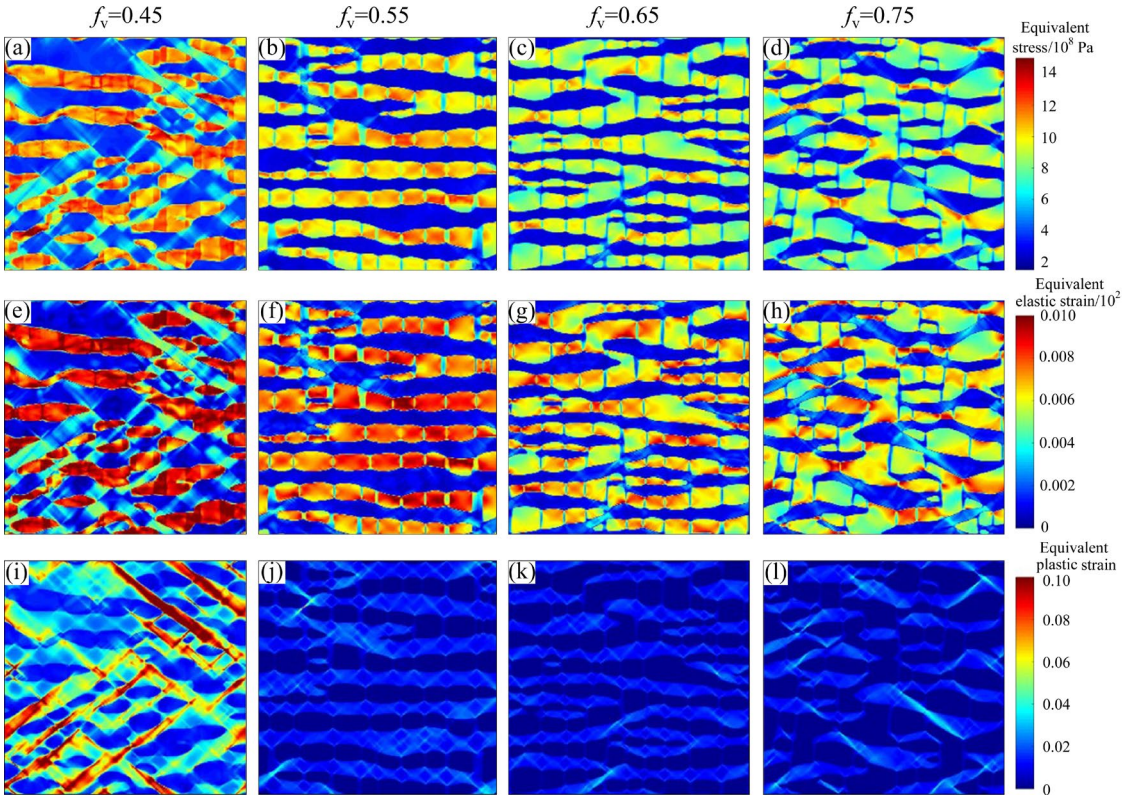

Fig. 8 Distributions of stress and strain field within γ' and γ phases at t=26.7 h for four cases: (a−d) Equivalent stress field; (e−h) Equivalent elastic strain field; (i−l) Equivalent plastic strain field

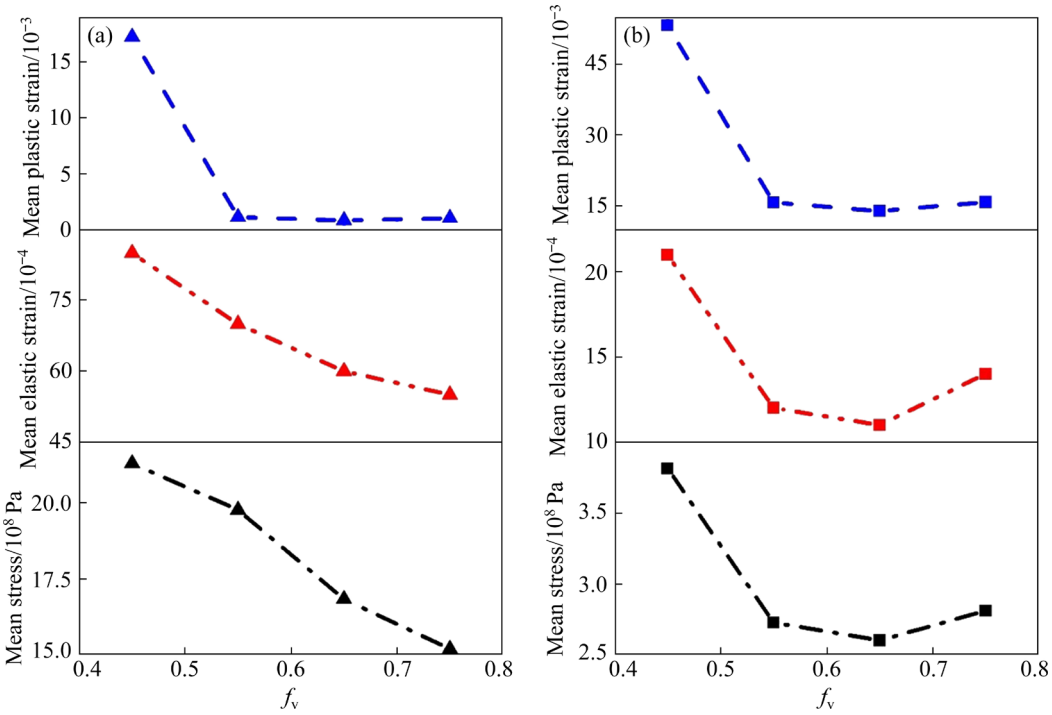

Fig. 9 Relationships between mean stress, mean elastic strain, mean plastic strain and f_v in γ' precipitate (a) and γ matrix (b) (t=26.7 h)

The changes of stress and strain fields with f_v can be attributed to the morphological changes of γ' and γ phases. As f_v increases from 0.45 to 0.65, the γ channels become narrower and the γ' rafts and γ channels formed during creep become more continuous (see Figs. 1(c, g, k) and Fig. 8). This continuous and narrow structure effectively hinders the dislocation movement and slows down the plastic deformation in γ channels. As a result, the mean plastic strain in γ channels decreases with increasing f_v. In addition, increased plastic deformation exacerbates creep damage which in turn enhances local stress concentration, resulting in a decrease of mean stress in γ channels with increasing f_v. Since elastic strain is proportional to stress, the mean elastic strain in γ channels also decreases with increasing f_v. Besides, the low plastic strain in γ channels causes low internal stress in γ' phases, leading to a decrease of mean stress in γ' phases with increasing f_v. In order for plastic deformation to occur in γ' phases, the resolved shear stress of γ' phases must be higher than the initial threshold. When there is a low accumulation rate of plastic strain in γ channels, a long time is needed to activate the plastic deformation in γ' phases, resulting a slower accumulation of plastic deformation. Therefore, the mean plastic strain in γ' phases decreases with increasing f_v. However, as f_v increases from 0.65 to 0.75, the γ channels become discontinuous and are isolated by the continuous γ' phases (see Figs. 1(o) and 8). Most discontinuous γ channels are inclined to the ⟨011⟩ directions and some γ channels are connected along these directions, which are beneficial for the movement of slip systems. As a result, the mean plastic strain in γ channels increases from f_v=0.65 to 0.75. Correspondingly, the mean stress and elastic strain in γ channels increase from f_v=0.65 to 0.75. Additionally, since the γ channels tilt towards the ⟨011⟩ directions when f_v=0.65, the dislocations can move for long distances and the obstructive effect of γ' phases is thus weakened but concentrated, resulting in low mean stress but high local stress concentration in γ' phases (see Fig. 8). This high local stress promotes plastic deformation in γ' phases, leading to an increase of mean plastic strain in γ' phases.

Because both stress and plastic strain in γ channels are in the lowest state when f_v=0.65, the steady-state creep rate is the lowest and the accumulation of creep damage is the slowest. In addition, the morphologies of γ' and γ phases in tertiary creep indicate that when f_v=0.65, the γ' rafts remain continuous and γ channels deviated to the

⟨011⟩ directions are short and narrow (see Fig. 1(l)), which are conducive to extending the tertiary creep. Under the combined influence of stress/strain evolution and γ'/γ morphology change, the creep life is the longest when f_v=0.65.

From above analysis, it can be concluded that the evolutions of stress and strain are closely linked to the microstructure morphologies, especially the γ channels where the plastic strain mainly occurs during the steady-state creep. Narrow and [010]-oriented γ channels exhibit strong resistance to the increase of internal stress and plastic strain. However, when γ channels are inclined towards the ⟨011⟩ directions, their resistance to plastic deformation is weakened. This suggests that under high f_v condition (e.g. f_v=0.75), if γ channels can be kept in the [010] direction during creep, the creep property can be improved efficiently. It should be noted that the appearance of [010]-oriented γ channels is a result of the formation of the [010]-oriented γ' rafts, and the stability of these channels depends on the stability of γ' rafts and γ'/γ interfaces. The formation of [010]-oriented γ' rafts is related to the elastic anisotropy of γ' phases. Since elastic anisotropy factor (ξ=C_{11}−C_{12}−2C_{44}) of γ' phases is negative, their elastically soft directions are ⟨001⟩, and the elastic energy is minimum when γ' phases (and γ'/γ interfaces) are aligned along the ⟨001⟩ directions [30]. For this reason, enhancing the elastic anisotropy can promote the preference for ⟨001⟩-oriented γ' rafts and potentially increase the stability of ⟨001⟩-oriented γ' rafts and γ channels. Therefore, designing γ' phases with strong elastic anisotropy is a promising approach to improving the creep properties of superalloys with high γ' volume fractions.

4.2 Distributions of creep damage under different f_v conditions

The creep damage is critical to the creep property. As plastic deformation accumulates, the amount of creep damage also increases. The areas with high levels of creep damage are more likely to develop cracks. The creep damage is accumulated on each slip system (see Eq. (10)). Figure 10 illustrates the distribution of creep damage on the $[1\bar{1}\bar{1}]\langle 101\rangle$ slip system after creep for different f_v cases. When f_v=0.45, the creep damage is mainly distributed in γ' phases. As f_v increases, the high levels of creep damage shift towards γ'/γ interfaces. When f_v=0.65, the creep damage is mainly distributed at the γ'/γ interfaces. As f_v continues to increase, the high levels of creep damage also appear in γ channels. MURAKUMO et al [7] indicated that Ni-SXs are strengthened through γ'/γ interfaces instead of γ' phases. Based on the current creep damage distribution, it can be inferred that when f_v is low, the SX is mainly strengthened by γ' phases, but their strengthening effect weakens with creep time. In the later stage of creep, γ' phases lose their strengthening effect due to the formation of a large amount of creep damage, which accelerates the creep fracture of the alloy. When f_v=0.65, the SX is mainly strengthened by γ'/γ interfaces, and the failure of this interface strengthening is one of the main reasons for fracture. When f_v is as high as 0.75, the strengthening effect of γ'/γ interfaces weakens, and there is a relatively higher creep damage distributed in the soft γ matrix compared to γ' phases.

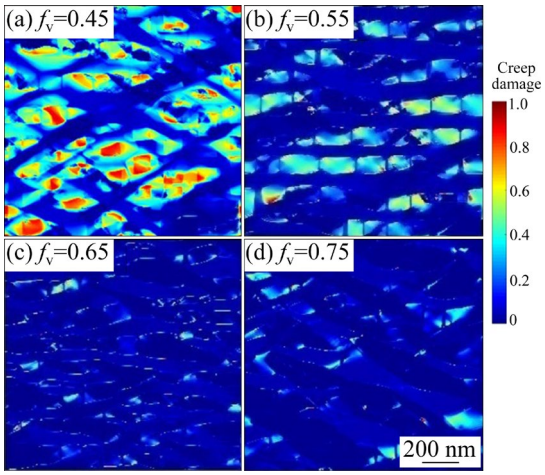

Fig. 10 Distribution of creep damage after creep at 1223 K, 300 MPa: (a) f_v=0.45; (b) f_v=0.55; (c) f_v=0.65; (d) f_v=0.75

5 Conclusions

(1) As f_v increases, the morphology of γ' rafts changes from discontinuous to continuous, opposite to the morphological change of γ channels; the inclination of γ channels from the [010] direction to the ⟨011⟩ directions in tertiary creep first decreases and then increases; steady-state creep rate, stress, elastic strain and plastic strain within γ channels in steady-state creep, also first decrease and then increase; the creep life first increases and then

decreases.

(2) When f_v=0.65, the steady-state creep rate is the lowest and the creep life is the longest, which is consistent with experimental results. This can be attributed to the microstructure and stress and strain fields. At this volume fraction, γ' rafts remain continuous, γ channels are slightly inclined to the ⟨011⟩ directions, and the stress and plastic strain in γ channels are in the lowest state, resulting in the lowest steady-state creep rate, slowest damage accumulation and thus the longest creep life.

(3) As f_v increases, the main distribution position of creep damage changes from γ' phases to γ'/γ interfaces and γ channels. When f_v=0.65, the creep damage is mainly distributed at γ'/γ interfaces.

(4) One possible approach to improving the creep properties of superalloys with a high γ' volume fraction is to enhance the elastic anisotropy of γ' phases.

CRediT authorship contribution statement

Min YANG: Conceptualization, Methodology, Writing − Original draft; **Fan YANG** and **Jia CHEN:** Software, Investigation, Visualization; **Min GUO:** Writing − Review & editing, Validation; **Hai-jun SU** and **Jun ZHANG:** Funding acquisition, Supervision, Resources.

Declaration of competing interest

The authors declare that they have no known competing financial interests or personal relationships that could have appeared to influence the work reported in this paper.

Acknowledgments

The authors would like to acknowledge the supports provided by the National Natural Science Foundation of China (Nos. 52301171, 52031012, 51971174), the National Science and Technology Major Project, China (Nos. 2019-VI-0020-0135), the Key Research and Development Program of Shaanxi Province, China (No. 2020ZDLGY13-02), and the Research Fund of the State Key Laboratory of Solidification Processing (NPU), China (No. 2022-TZ-01).

References

[1] CARON P, RAMUSAT C, DIOLOGENT F. Influence of the γ' fraction on the γ/γ' topological inversion during high temperature creep of single crystal superalloys [C]//Proc Superalloys 2008. Warrendale, PA: TMS, 2008: 159−167.

[2] MUKHERJI D, RÖSLER J. Effect of the γ' volume fraction on the creep strength of Ni-base superalloys [J]. Zeitschrift für Metallkunde, 2003, 94: 478−484.

[3] POLLOCK T M, ARGON A S, Creep resistance of CMSX-3 nickel base superalloy single crystals [J]. Acta Metallurgica et Materialia, 1992, 40: 1−30.

[4] SHI Zhen-xue, LI Jia-rong, LIU Shi-zhong, WANG Xiao-guang. Creep properties and microstructure evolution of nickel-based single crystal superalloy at different conditions [J]. Transactions of Nonferrous Metals Society of China, 2014, 24: 2536−2543.

[5] YUE Quan-zhao, LIU Lin, YANG Wen-Chao, HUANG Tai-wen, ZHANG Jun, FU Heng-zhi. Stress dependence of dislocation networks in elevated temperature creep of a Ni-based single crystal superalloy [J]. Materials Science and Engineering A, 2019, 742: 132−137.

[6] NATHAL M V. Effect of initial gamma prime size on the elevated temperature creep properties of single crystal nickel base superalloys [J]. Metallurgical Transactions A, 1987, 18: 1961−1970.

[7] MURAKUMO T, KOBAYASHI T, KOIZUMI Y, HARADA H. Creep behaviour of Ni-base single-crystal superalloys with various γ' volume fraction [J]. Acta Materialia, 2004, 52: 3737−3744.

[8] PYCZAK F, NEUMEIER S, GÖKEN M. Influence of lattice misfit on the internal stress and strain states before and after creep investigated in nickel-base superalloys containing rhenium and ruthenium [J]. Materials Science and Engineering A, 2009, 510/511: 295−300.

[9] HARADA H, YAMAZAKI M, KOIZUMI Y, SAKUMA N, FURUYA N, KAMIYA H. Alloy design for nickel-base superalloys [C]//Proc High Temperature Alloys for Gas Turbines 1982. Belgium, PA: Springer Netherlands, 1982: 721−735.

[10] RO Y, KOIZUMI Y, HARADA H. High temperature tensile properties of a series of nickel-base superalloys on a γ/γ' tie line [J]. Materials Science and Engineering A, 1997, 223: 59−63.

[11] WU Rong-hai, YUE Zhu-feng, WANG Meng. Effect of initial γ/γ' microstructure on creep of single crystal nickel-based superalloys: A phase-field simulation incorporating dislocation dynamics [J]. Journal of Alloys and Compounds, 2019, 779: 326−334.

[12] YU Zhi-yuan, WANG Xin-mei, YANG Fu-qian, YUE Zhu-feng, LI James C M. Review of γ' rafting behavior in nickel-based superalloys: Crystal plasticity and phase-field simulation [J]. Crystals, 2020, 10: 1095.

[13] ZHOU Ning, SHEN Chen, MILLS M, WANG Yun-zhi. Large-scale three-dimensional phase field simulation of γ'-rafting and creep deformation [J]. Philosophical Magazine, 2010, 90: 405−436.

[14] COTTURA M, BOUAR Y L, FINEL A, APOLAIRE B, AMMAR K, FOREST S. A phase field model incorporating strain gradient viscoplasticity: Application to rafting in Ni-base superalloys [J]. Journal of the Mechanics and Physics of Solids, 2012, 60: 1243−1256.

[15] TSUKADA Y, KOYAMA T, MURATA Y, MIURA N, KONDO Y. Estimation of γ/γ' diffusion mobility and three-dimensional phase-field simulation of rafting in a

commercial nickel-based superalloy [J]. Computational Materials Science, 2014, 83: 371−374.
[16] ZHOU N, SHEN C, MILLS M J, WANG Y. Phase field modeling of channel dislocation activity and γ′ rafting in single crystal Ni−Al [J]. Acta Materialia, 2007, 55: 5369−5381.
[17] COTTURA M, APPOLAIRE B, FINEL A, BOUAR Y Le. Coupling the phase field method for diffusive transformations with dislocation density-based crystal plasticity: Application to ni-based superalloys [J]. Journal of the Mechanics and Physics of Solids, 2016, 94: 473−489.
[18] YANG Min, ZHANG Jun, WEI Hua, GUI Wei-min, SU Hai-jun, JIN Tao, LIU Lin. A phase-field model for creep behavior in nickel-base single-crystal superalloy: Coupled with creep damage [J]. Scripta Materialia, 2018, 147: 16−20.
[19] YANG Min, ZHANG Jun, GUI Wei-min, HU Song-song, LI Zhuo-ran, GUO Min, SU Hai-jun, LIU Lin. Coupling phase field with creep damage to study γ′ evolution and creep deformation of single crystal superalloys [J]. Journal of Materials Science & Technology, 2021, 71: 129−137.
[20] CHEN Jia, GUO Min, YANG Min, LIU Lin, ZHANG Jun. Double minimum creep processing and mechanism for γ′ strengthened cobalt-based superalloy [J]. Journal of Materials Science & Technology, 2022, 112: 123−129.
[21] WU Rong-hai, ZHANG Yu-fan. Phase-field, dislocation based plasticity and damage coupled model: Modelling and application to single crystal superalloys [J]. International Journal of Plasticity, 2022, 157: 103376.
[22] MÉRIC L, POUBANNE P, CAILLETAUD G. Single crystal modeling for structural calculations: Part 1−Model presentation [J]. Journal of Engineering Materials and Technology, 1991, 113: 162−170.
[23] VLADIMIROV I N, REESE S, EGGELER G. Constitutive modelling of the anisotropic creep behaviour of nickel-base single crystal superalloys [J]. International Journal of Mechanical Sciences, 2009, 51: 305−313.
[24] TANAKA K, ICHITSUBO T, KISHIDA K, INUI H, MATSUBARA E. Elastic instability condition of the raft structure during creep deformation in nickel-base superalloys [J]. Acta Materialia, 2008, 56: 3786−3790.
[25] ALI M A, AMIN W, SHCHYGLO O, STEINBACH I. 45-degree rafting in Ni-based superalloys: A combined phase-field and strain gradient crystal plasticity study [J]. International Journal of Plasticity, 2020, 128: 102659.
[26] TOURATIER F, ANDRIEU E, POQUILLON D, VIGUIER B. Rafting microstructure during creep of the MC_2 nickel-based superalloy at very high temperature [J]. Materials Science and Engineering A, 2009, 510/511: 244−249.
[27] KAMARAJ M, MAYR C, KOLBE M, EGGELER G. On the influence of stress state on rafting in the single crystal superalloy CMSX-6 under conditions of high temperature and low stress creep [J]. Scripta Materialia, 1998, 34: 589−594.
[28] MÜLLER L, GlATZEL U, FELLER-KNIEPMEIER M. Calculation of the internal stresses and strains in the microstructure of a single crystal nickel-base superalloy during creep [J]. Acta Metallurgica et Materialia, 1993, 41: 3401−3411.
[29] SULZER S, LI Z, ZAEFFERER S, HAGHIGHAT S M H, WILKINSON A, RAABE D, REED R. On the assessment of creep damage evolution in nickel-based superalloys through correlative HR-EBSD and cECCI studies [J]. Acta Materialia, 2020, 185: 13−27.
[30] DOI M. Elasticity effects on the microstructure of alloys containing coherent precipitates [J]. Progress in Materials Science, 1996, 40: 79−180.

基于相场模拟的镍基高温合金γ′相体积分数对蠕变性能的影响机理

杨 敏，杨 帆，陈 佳，郭 敏，苏海军，张 军

西北工业大学 凝固技术国家重点实验室，西安 710072

摘 要：γ′相体积分数(f_v)对镍基单晶高温合金的力学性能起着至关重要的作用。采用蠕变相场模型，模拟不同 f_v 条件下蠕变过程中的显微组织演化和蠕变性能。通过分析应力场和应变场演化，研究 γ′相体积分数对蠕变性能的影响机制。随着 f_v 的增加，γ′筏的形态从不连续变为连续，与 γ 通道的形态变化正好相反；蠕变第 3 阶段时 γ 通道由[010]方向向⟨011⟩方向的倾斜程度先减小后增大；蠕变寿命先增大后减小；蠕变损伤的主要分布位置从 γ′相向 γ′/γ 界面和 γ 通道转移。f_v=0.65 时蠕变寿命最长，这是因为在此条件下 γ′筏结构最稳定、γ 通道中应力和应变量最低以及损伤累积最慢。

关键词：相场模拟；内应力；内应变；蠕变行为；单晶高温合金

(Edited by Bing YANG)